ELSEVIER

Biophysical Chemistry 67 (1997) 35–41

Biophysical Chemistry

Two-photon excitation of ethidium bromide labeled DNA [1]

Henryk Malak, Felix N. Castellano, Ignacy Gryczynski, Joseph R. Lakowicz *

Center for Fluorescence Spectroscopy, Department of Biochemistry and Molecular Biology, University of Maryland School of Medicine, 725 W. Lombard Street, Baltimore, MD 21201, USA

Received 18 December 1996; revised 13 January 1997; accepted 13 January 1997

Abstract

We examined the steady state and time-resolved emission of DNA stained with ethidium bromide (EB) when excited with 90 fs pulses from a mode-locked titanium sapphire laser. Over the wavelength range from 840 to 880 nm EB–DNA was found to display two-photon excitation, with a cross-section near 7×10^{-50} cm^4s/photon. Frequency-domain intensity decay measurements revealed similar multi-exponential intensity decays for one- and two-photon excitation. Time-resolved anisotropy decay measurements revealed similar correlation times, but different amplitudes as has been observed previously for two- versus one-photon excitation. These results indicate that two-photon excitation of EB–DNA can be accomplished with the fundamental output of a Ti:sapphire laser without obvious heating or perturbation of the DNA. © 1997 Elsevier Science B.V.

Keywords: Fluorescence spectroscopy; Fluorescence microscopy; Imaging; Time-resolved fluorescence; Two-photon excitation; Three-photon excitation; DNA; Ethidium bromide; Chromosomes; Multi-photon microscopy

1. Introduction

Two-photon spectroscopy has been used to understand the symmetry of molecular excited states [1–3]. The increasing availability of fs laser sources with high peak power has resulted in a renewed interest in multi-photon excitation of biochemical fluorophores. Two- [4–11] and three-photon [12–16] excitation has been observed for a variety of fluorophores. Two-photon [17,18] and three-photon [19–21] excitation has been applied to microscopic imaging where the quadratic or cubic dependence on the light intensity results in strongly localized excitation and the equivalent of confocal imaging. The localized excitation obtained with multi-photon excitation has been used for localized photolysis in neuronal tissues [22] and for selective excitation of adjacent fluorophores in scattering media [23].

Ethidium bromide (EB) is one of the most widely used stains for DNA in fluorescence microscopy. This widespread usage is the result of its favorable properties of being weakly fluorescent in aqueous solution, and highly fluorescent when intercalated into double helical DNA [24,25]. EB binding to DNA does not appear to be base pair specific, and the emission spectra, quantum yields and decay times

Abbreviations: DAPI, 4′,6-diamidino-2-phenylindole,hydrochloride; EB, Ethidium bromide; Hoechst 33342, bis-benzimide, 2,5′-bi-1H-benzimidazole, or 2′-(4-ethoxyphenyl)-5-(4-methyl-1-piperazinyl); 1PE, 2PE or 3PE, one-, two- or three-photon excitation, respectively; FD, frequency-domain

* Corresponding author.

[1] Dedicated to Professor Alfons Kawski on the occasion of his 70th birthday.

PII S0301-4622(97)00017-3

are similar irrespective of the adjacent base pairs. However, in spite of the widespread interest in multi-photon spectroscopy and imaging, no information is available on the spectral properties of EB–DNA with multi-photon excitation. The only report is the two-photon excitation spectrum recently reported by Webb and colleagues [26]. In the present report we describe the steady state and time-resolved fluorescent spectral properties of EB–DNA with two-photon excitation.

2. Materials and methods

Calf thymus DNA was obtained from Sigma and used without further purification. EB was obtained from Sigma, EB–DNA was prepared by mixing appropriate quantities of EB and DNA in aqueous buffer, 10 mM tris, pH 8, containing 100 mM NaCl. The concentration of EB was determined using a molar extinction coefficient of $\epsilon = 5350\ M^{-1}\ cm^{-1}$ at 483 nm. The concentration of DNA base pairs was determined using $\epsilon = 13\,500\ M^{-1}\ cm^{-1}$ at 259 nm. The EB to DNA base pair ratio was 1:50.

All fluorescence spectral measurements were performed in the apparatus shown in Scheme 1. The excitation source was a mode-locked Ti:sapphire laser from Spectra Physics, providing approximate 90 fs pulses at 80 MHz, with an average power near 800 mW. The 840 to 880 nm excitation was passed through a Spectra Physics pulse picker to decrease the repetition rate to 4 MHz. This allows time-resolved frequency-domain measurements at integer multiplies of the 4 MHz repetition rate [27–29]. For

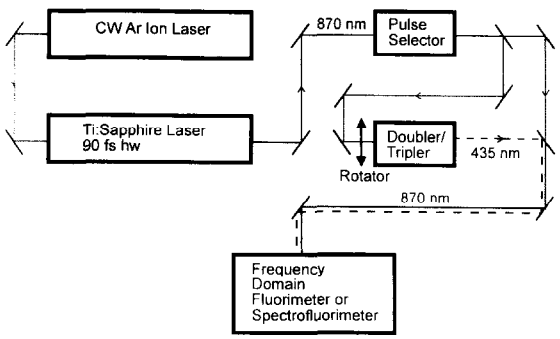

Scheme 1. Experimental apparatus for one- and two-photon excitation of EB–DNA.

multi-photon excitation the pulse-selected Ti:sapphire output was taken directly to the sample. For one-photon excitation the fundamental pulses were frequency-doubled using an Inrad doubler–tripler yielding an average power of 200 mW at 80 MHz and 10 mW at 4 MHz, respectively. The excitation was vertically polarized. For multi-photon excitation the laser fundamental was focused using a 2-cm focal lens, providing a spot size near 20 μm in diameter, and a peak intensity near $3 \times 10^{10}\ W/cm^2$.

Frequency-domain intensity and anisotropy decays were measured as described previously [29,30]. For 1PE excitation the emission was isolated using a 500 nm Andover cutoff filter to eliminate scattered light. For 2PE excitation the emission was isolated with a short pass filter transmitting below 750 nm (Corning heat filter 03FHA023). Intensity decays were measured using magic angle polarization conditions. Because of the poor response of our photomultiplier tube above 800 nm, intensity decays were measured using a reference fluorophore of known lifetime [31]. We used DCM in ethanol as the reference with an assumed single exponential decay time of 1.81 ns. DCM displayed two-photon excitation at 820–880 nm and one-photon excitation at 410 to 440 nm.

Frequency-domain intensity and anisotropy data with multi-photon excitation were analyzed as described previously for one-photon excitation [30,32]. The intensity decay was assumed to be multi-exponential

$$I(t) = \sum_{i=1}^{n} \alpha_i e^{-t/\tau_i} \tag{1}$$

where α_i are the preexponential factors, τ_i are the decay times, and n number of exponential components. The fractional intensity of each component in the steady state emission is given by

$$f_i = \frac{\alpha_i \tau_i}{\sum_j \alpha_j \tau_i} \tag{2}$$

The mean lifetime is given by $\bar{\tau} = \sum_j f_j \tau_j$. In frequency-domain fluorometry, the sample is excited with an intensity-modulated light source, in the present case the output of a mode-locked Ti:sapphire laser. The phase angle (θ_ω) and the modulation (m_ω) of the emission are related to the intensity decay

parameters, α_i and τ_i, and modulation frequency ω by

$$\phi_\omega = \arctan(N_\omega/D_\omega),\ m_\omega = \left(N_\omega^2 + D_\omega^2\right)^{1/2} \qquad (3)$$

where

$$N_\omega = \frac{1}{J}\sum_{i=1}^{n}\frac{\omega\alpha_i\tau_i^2}{1+\omega^2\tau_i^2},\ D_\omega = \frac{1}{J}\sum_{i=1}^{n}\frac{\alpha_i\tau_i}{1+\omega^2\tau_i^2}$$

$$J = \sum_{i=1}^{n}\alpha_i\tau_i \qquad (4)$$

The values α_i and τ_i are determined by minimization of the goodness-of-fit parameter

$$\chi_R^2 = \frac{1}{\nu}\sum_{\omega,k}\left(\frac{\phi_\omega - \phi_{\omega c}}{\delta\phi}\right)^2 + \frac{1}{\nu}\sum_{\omega,k}\left(\frac{m_\omega - m_{\omega c}}{\delta m}\right)^2 \qquad (5)$$

where the subscript c indicates calculated values for known values of α_i and τ_i, $\delta\phi$ and δm the experimental uncertainties in the measured phase and modulation values, and ν is the number of degrees of freedom.

The hydrodynamics of DNA are complex, and analysis of the anisotropy decay of labeled DNA requires the use of appropriate models [33–35]. The objective of the present report is not to advance this theory [33–35]. Instead, we use the anisotropy decays to detect the effects of intense illumination on the conformation and dynamics of DNA. Hence, the frequency-domain anisotropy decays were analyzed in terms of the multi-correlation time model

$$r_k(t) = \sum_j r_{jk}\, e^{-t/\theta_{jk}} \qquad (6)$$

where θ_j is the rotational correlation time displaying an amplitude r_{jk} in the anisotropy decay. The subscript k indicates the mode of excitation (1PE, 2PE or 3PE). In the absence of optical effects on DNA dynamics we expect the correlation time (θ_j) to be independent of the mode of excitation. However, based on previous studies of DAPI [10] and Hoechst 33342 [11] with 1PE and 2PE excitation the amplitudes (r_{jk}) are expected to depend on the nature of the excitation process. The value of r_{jk} and θ_j are recovered by least squares analysis of the differential polarized phase angles and modulated anisotropies [32], using an expression similar to Eq. (4). For the global analysis the same correlation times were used for each excitation wavelength (k), and the r_{jk} values were distinct for each wavelength. The sum in Eq. (5) extends over the excitation wavelengths, where it is understood that phase and modulation data are available for two excitation wavelengths. The time-zero anisotropy is given by the sum of the amplitudes, $r_{0k} = \sum_j r_{jk}$.

3. Fluorescence anisotropy with multi-photon excitation

The time-zero anisotropy is a measure of the displacement of the emission transition moment from the direction of the polarized excitation. The theory for the expected r_{0k} values for two-photon excitation is complex [36–39], and analogous theories for 3 hν excitation are not yet available. However, we have found that for many fluorophores the anisotropy behavior can be understood in terms of polarized photoselection with collinear transitions for the 2PE and 3PE transitions. In these cases the time-zero anisotropy is given by

$$r_{01}(\beta) = \frac{2}{5}\left(\frac{3}{2}\cos^2\beta_1 - \frac{1}{2}\right) \qquad (7)$$

$$r_{02}(\beta) = \frac{4}{7}\left(\frac{3}{2}\cos^2\beta_2 - \frac{1}{2}\right) \qquad (8)$$

$$r_{03}(\beta) = \frac{2}{3}\left(\frac{3}{2}\cos^2\beta_3 - \frac{1}{2}\right) \qquad (9)$$

for 1PE, 2PE and 3PE excitation, respectively. The factors $\frac{2}{5}$, $\frac{4}{7}$ and $\frac{2}{3}$ originate with $\cos^2\theta$, $\cos^4\theta$ and $\cos^6\theta$ photoselection, where θ is the angle between the excitation polarization and the transition moment of the molecule. The angle β_k is the angular displacement between the absorption and emission transition, and need not be identical for each mode of excitation (k). More specifically, if the effective β for one-, two- and three-photon excitation are identical, then the time-zero anisotropies will be related by Eqs. (7)–(9). However, fluorophores can display more complex behavior, as has already been observed for tryptophan derivatives and proteins [7,8,36].

For one-, two- and three-photon excitation the maximal anisotropies for $\beta_k = 0°$ are 0.40, 0.571 and 0.667, respectively. Observation of a larger anisotropy for three- versus two-photon excitation provides strong evidence for three-photon excitation. We note that the above description is somewhat simplified, and that multi-photon transitions are more correctly described as tensors [36–39]. For the present data the simple theory described in Eqs. (7)–(9) is adequate for interpretation of the results.

4. Results

Emission spectra of EB are shown in Fig. 1 for one-photon excitation at 435 nm. In the absence of DNA the emission is weak, and the intensity of EB increases about 20-fold upon binding to double helical DNA. Also shown in Fig. 1 is the emission spectra of EB–DNA for excitation at 870 nm. At this wavelength excitation must be the result of a multi-photon process as the energy of a single 870 nm photon is not adequate to reach the lowest singlet state of EB. The same emission spectra were observed for 1PE at 435 nm and multi-photon excitation at 870 nm. This result agrees with the consistent observations to date of the same emission spectra for fluorophores independent of the mode of excitation [5–11,26].

To determine the mode of excitation of EB–DNA we measured the dependence of the emission intensity on laser power at 435 and 870 nm (Fig. 2). At

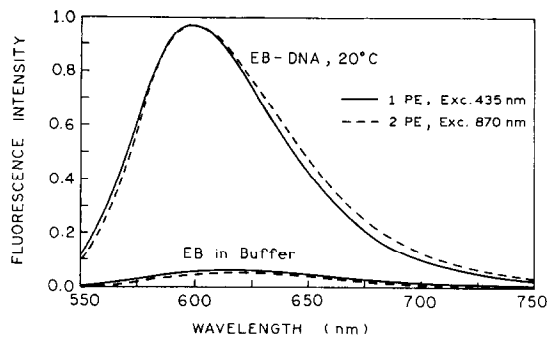

Fig. 1. Emission spectra of ethidium bromide in water and bound to DNA for 1PE at 435 nm [EB] = 40 μM, [DNA base pairs] = 2 mM. Also shown are the emission spectra observed for excitation at 870 nm (– – –).

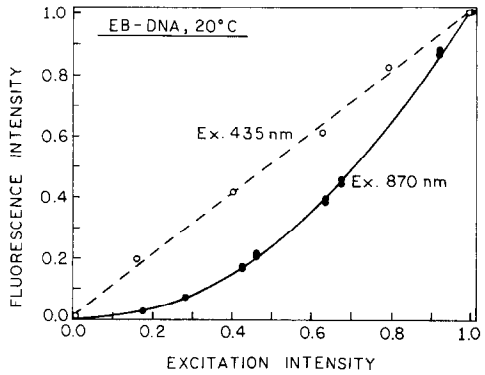

Fig. 2. Dependence of the emission intensity of EB–DNA on laser power, normalized to the highest incident intensity. The maximum intensity at 870 nm was 40 mW, and 10 mW at 435 nm, and the pulse repetition rate was 4 MHz.

870 nm the dependence is obviously quadratic. A plot of log emission intensity versus laser power yield a slope of 2.0. Hence, EB–DNA displays two-photon excitation at 870 nm. Similar results indicating 2PE excitation were observed from 820 to 880 nm.

We estimated the cross-section for two-photon excitation of EB–DNA by comparison of its intensity with that of Rhodamine B (RhB) in water. For this comparison we used a RhB two-photon cross-section of 40×10^{-50} cm^4 s/photon at 870 nm [26]. Using estimated quantum yields of 0.13 for EB–DNA and 0.48 for RhB we estimated the two-photon cross-section of EB–DNA to be 6.7×10^{-50} cm^4 s/photon.

The intensity and anisotropy decays of fluorophores are known to be sensitive indicators of the conformation of biomolecules. This is particularly true for EB–DNA. In this case disruption of the DNA double helix due to the intense illumination used for 2PE would be expected to displace EB from the helix, resulting in shorter lived components in the intensity and/or anisotropy decays. Frequency-domain intensity decays are shown in Fig. 3, and the parameters of the multi-exponential analysis are summarized in Table 1. The frequency domain data are visually nearly identical (Fig. 3), an impression confirmed by the least squares analysis. Similar amplitude and decay times were obtained for 1PE and 2PE (Table 1).

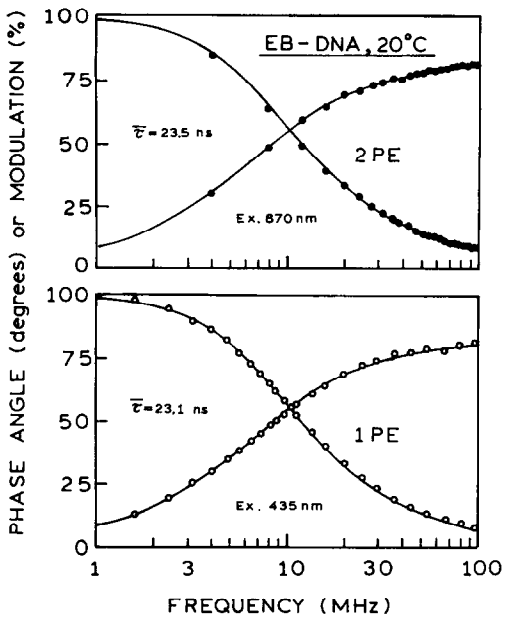

Fig. 3. Frequency-domain intensity decay of EB–DNA for 2PE at 870 nm (top) and for 1PE at 435 nm (bottom).

To further test the similarity of the intensity decays we analyzed the 435 and 870 nm data globally using the same intensity decay law. This analysis (Table 1) resulted in a good fit to both sets of data, without a significant elevation of the goodness-of-fit parameter χ_R^2. This result indicates that within our experimental resolution the same decay law describes the intensity decay with 1PE and 2PE excitation.

Table 1
Multi-exponential intensity decays of ethidium bromide–DNA, pH = 8.0, 20°C

Excitation (nm)	τ_1 (ns)	Range (ns)[c]	f_i	χ_R^2
435 nm	1.54	1.10–1.93	0.01	
	22.86	22.67–23.05	0.99	2.8[a]
870 nm	2.31	2.11–2.53	0.02	
	23.54	23.26–23.83	0.98	1.3[b]
435 and 870 nm	1.96	1.74–2.19	0.02	
Global	23.89	22.71–23.64	0.98	2.5

[a] The values of χ_R^2 for the single and triple exponential fit were 28.2 and 2.2 respectively. The errors in phase and modulation were taken as 0.3° and 0.007 for all analyses.
[b] The values of χ_R^2 for the single and triple exponential fits were 61.4 and 1.4 respectively.
[c] The range of values consistent with the data were calculated according to [41].

Anisotropy decays provide a sensitive indicator of the hydrodynamics and flexibility of biomolecules. Hence we examined the anisotropy decay of EB–DNA with 435 and 870 nm excitation (Fig. 4). These data reveal a similar shape to the differential polarized phase (top) and modulated anisotropy data (bottom), but different magnitudes. Least-squares analysis reveals that the time-zero amplitudes are elevated for excitation at 870 nm as compared to 435 nm excitation (Table 2). The total time-zero anisotropies are 0.22 and 0.28 for 1PE and 2PE, respectively. In previous studies [40] we have shown that for similar orientation of the 1PE and 2PE one can expect the anisotropies to be in the ratio of 1:1.43. In the case of EB–DNA we observed a ratio of 1:1.27. Hence it appears that these are somewhat different orientations of the excitation moment relative to the emission moment for 1PE and 2PE excitation, or that there are non-zero off diagonal elements in the two-photon transition tensor. The 2PE transition are more properly described as tensors [36], and the orientation and nature of the 2PE tensors can affect the time-zero anisotropy.

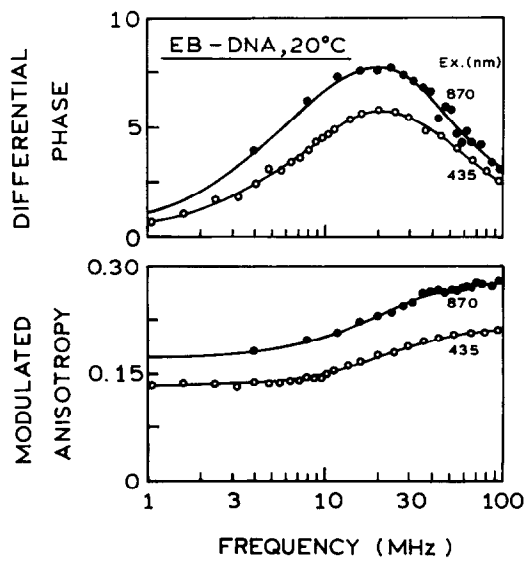

Fig. 4. Frequency-domain anisotropy decay of EB–DNA for 2PE at 870 nm (●) and for 1PE at 435 nm (○).

Table 2
Multi-exponential anisotropy decay analysis of ethidium bromide–DNA, pH = 8.0, 20°C

Excitation (nm)	θ_i (ns)	Range (ns)[c]	r_i	χ_R^2
435 nm	8.8	8.4–9.3	0.10	
	217	175–267	0.12	1.3[a]
870 nm	9.1	8.1–10.6	0.12	
	126	83–192	0.16	3.9[b]
435 and 870 nm	10	9.4–11.0	0.11	2.5
Global	248	157–390	0.11	

[a]The values of χ_R^2 for the single and triple exponential fit were 2.6 and 4.7 respectively. The errors in phase and modulation were taken as 0.3° and 0.007 for all analyses.
[b]The values of χ_R^2 for the single and triple exponential fits were 42.5 and 4.2 respectively.
[c]The range of values consistent with the data were calculated with consideration of parameter correlation [41].

Close examination of the FD anisotropy decays of EB–DNA (Fig. 4) reveals a modest shift of the differential phase data (top) to lower frequencies. However, least squares analysis reveals similar correlation times for one- and two-photon excitation (Table 2), particularly if one considers the uncertainties in the recovered correlation times. Global analysis of the FD anisotropy decays with the same correlation time, but different time-zero amplitudes, resulted in a good fit (Table 2). Hence the data suggest a modest heating effect in DNA with 2PE excitation, but the results do not unequivocally demonstrate such an effect.

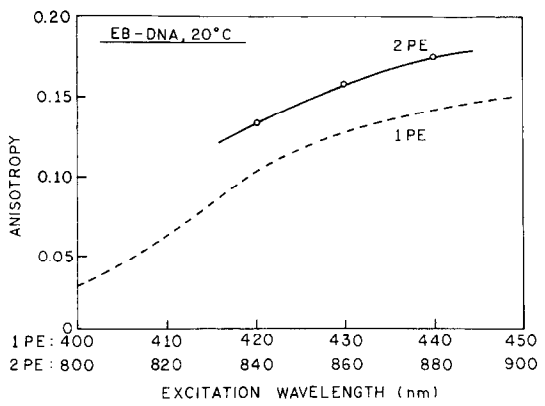

Fig. 5. Steady state anisotropy of EB–DNA with 1PE and 2PE excitation.

To further examine the relationship of the 1PE and 2PE anisotropies we examined the wavelength-dependent steady state anisotropies of EB–DNA. The measured anisotropy for two-photon excitation was higher than for one-photon excitation (Fig. 5). The wavelength-dependent steady state anisotropies appear to be dependent on excitation wavelength and changes in the same manner for one- and two-photon excitation of EB–DNA.

5. Discussion

In recent years we have observed the increased experimental possibilities resulting from high repetition rate dye lasers. This trend has continued with the introduction of mode-locked Ti:sapphire lasers, which are simpler to operate than dye lasers and provide shorter pulse widths near 100 fs. However, the fundamental output of the Ti:sapphire lasers is maximal from 800 to 900 nm, which is too long for one-photon excitation of many biochemical fluorophores.

The Ti:sapphire laser can be operated at its most efficient wavelength near 850 nm which is suitable for multi-photon excitation of the DNA stains as EB, DAPI and Hoechst 33342. The mode of excitation for these last two stains can be changed from 2PE to 3PE with modest changes in wavelength [21]. The possibility of three-photon excitation in bioimaging has already been accomplished for a DAPI at 970 nm by using a Ti:sapphire laser [21]. Remarkably, images were obtained without dielectric breakdown of the samples. Hence it appears that multi-photon imaging is possible with modern fs lasers.

The data in this report suggests that two-photon excitation of EB can be used to study DNA dynamics and to study chromosomes. The observed higher anisotropy of EB for two-photon excitation compared to one-photon excitation allows for greater accuracy in measurements of DNA dynamics and an increase in sensitivity of biochemical polarization assays.

Acknowledgements

This work was supported by NIH National Center for Research Resources RR-08119. FNC is supported by a NIH postdoctoral fellowship (GM 18653).

References

[1] M.J. Wirth, A. Koskelo, M.J. Sanders, Appl. Spectroscopy 35 (1) (1981) 14–21.
[2] M.J. Wirth, F.E. Lytle, Anal. Chem. 49 (1997) 2954–2961.
[3] D.M. Friedrich, W.M. McClain, Ann. Rev. Phys. Chem. 31 (1980) 559–577.
[4] D.M. Sammeth, S. Yan, L.H. Spangler, P.R. Callis, J. Phys. Chem. 94 (1990) 7340–7342.
[5] J.R. Lakowicz, I. Gryczynski, E. Danielsen, J.K. Frisoli, Chem. Phys. Lett. 194 (1992) 282–287.
[6] A.R. Rehms, P.R. Callis, Chem. Phys. Lett. 208 (3,4) (1993) 276–282.
[7] J.R. Lakowicz, I. Gryczynski, Biophys. Chem. 45 (1993) 1–6.
[8] J.R. Lakowicz, B. Kierdaszuk, P.R. Callis, H. Malak, I. Gryczynski, 1996. Biophys. Chem., in press.
[9] J.R. Lakowicz, I. Gryczynski, J. Kuśba, E. Danielsen, J. Fluoresc. 2 (1992) 247–258.
[10] J.R. Lakowicz, I. Gryczyński, J. Fluoresc. 2 (1992) 117–122.
[11] I. Gryczynski, J.R. Lakowicz, J. Fluoresc. 4 (1994) 331–336.
[12] I. Gryczynski, H. Malak, J.R. Lakowicz, Biospectroscopy 2 (1996) 9–15.
[13] H. Malak, I. Gryczynski, J.D. Dattelbaum, J.R. Lakowicz, 1996. J. Fluoresc., in press.
[14] I. Gryczynski, H. Szmacinski, J.R. Lakowicz, Photochem. Photobiol. 62 (4) (1995) 804–808.
[15] H. Szmacinski, I. Gryczynski, J.R. Lakowicz, Biophys. J. 70 (1996) 547–555.
[16] I. Gryczynski, H. Malak, J.R. Lakowicz, Chem. Phys. Letts. 245 (1995) 30–35.
[17] W. Denk, J.H. Strickler, W.W. Webb, Science 248 (1990) 73–76.
[18] W.W. Webb, MICRO 90 (London) 13 (1990) 445–450.
[19] S.W. Hell, K. Bahlmann, M. Schrader, A. Soini, H. Malak, I. Gryczynski, J.R. Lakowicz, J. Biomed. Optics 1 (1) (1996) 71–74.
[20] I. Gryczynski, H. Malak, S.W. Hell, J.R. Lakowicz, J. Biomed. Optics 1 (4) (1996) 473–480.
[21] J.R. Lakowicz, I. Gryczynski, H. Malak, M. Schrader, P. Engelhardt, H. Kano, S.W. Hell, Biophy. J. 72 (1997) 567–578.
[22] W. Denk, K.R. Delaney, A. Gelperin, D. Kleinfeld, B.W. Strowbridge, D.W. Tank, R. Yuste, J. Neuros. Meth. 54 (1994) 151–152.
[23] H. Szmacinski, I. Gryczynski, J.R. Lakowicz, 1996. Proc. Nat. Acad. Sci. USA, submitted.
[24] J.C. Thomas, J.M. Schurr, Biochem. 22 (1983) 6194–6198.
[25] M.E. Hogan, O. Jardetzky, Biochemistry 19 (1980) 2079–2085.
[26] C. Xu, W.W. Webb, J. Opt. Soc. Am. 13 (1996) 481–491.
[27] K. Berndt, H. Cuerr, D. Palme, Opt. Commun. 42 (1982) 419–422.
[28] E. Gratton, D.M. Jameson, R.D. Hall, Ann. Rev. Biophys. Bioeng. 13 (1984) 105–124.
[29] G. Laczko, J.R. Lakowicz, I. Gryczynski, Z. Gryczynski, H. Malak, Rev. Sci. Instrum. 61 (1990) 2331–2337.
[30] J.R. Lakowicz, I. Gryczynski, in: J.R. Lakowicz (Ed.), Topics in Fluorescence Spectroscopy, Vol. 1: Techniques, Plenum Press, New York, 1991, pp. 293-355.
[31] J.R. Lakowicz, H. Cherek, A. Balter, J. Biochem. Biophys. Meth. 5 (1981) 131–146.
[32] J.R. Lakowicz, H. Cherek, J. Kuśba, I. Gryczynski, M.L. Johnson, J. Fluoresc. 3 (1993) 103–116.
[33] J.M. Schurr, B.S. Fujimoto, P. Wu, L. Song, in: J.R. Lakowicz (Ed.), Topics in Fluorescence Spectroscopy, Vol. 3: Biochemical Applications, Plenum Press, New York, 1992, pp. 137-229.
[34] D.P. Millar, R.J. Robbins, A.H. Zewail, J. Chem. Phys. 76 (1982) 2080–2094.
[35] M.D. Barkley, B.H. Zimm, J. Chem. Phys. 70 (1979) 2991–3007.
[36] P.R. Callis, J. Chem. Phys. 99 (1) (1993) 27–37.
[37] S.-Y. Chen, B.W. Van Der Meer, Biophys. J. 64 (1993) 1567–1575.
[38] C. Wan, C.K. Johnson, Chem. Phys. 179 (1994) 513–531.
[39] C. Wan, C.K. Johnson, J. Chem. Phys. 101 (1994) 10283–10291.
[40] I. Gryczynski, H. Malak, J.R. Lakowicz, Chem. Phys. Letts. 245 (1995) 30–35.
[41] M. Straume, S.G. Frasier-Cadoret, M.L. Johnson, in: J.R. Lakowicz (Ed.), Topics in Fluorescence Spectroscopy, Vol. 3: Principles, Plenum Publishing, New York, 1991, pp. 177-240.